(2)

Office of Naval Research
Contract N00014-88-K-0472
R T Code 413p008

Technical Report No. 1

A Molecular Mechanics Analysis of Molecular Recognition By Cyclodextrin Mimics of Alpha-Chymotrypsin

by

C.A. Venanzi, P.M. Canzius, Z. Zhang, and J.D. Bunce

To Be Published in

The Journal of Computational Chemistry

New Jersey Institute of Technology
Chemistry Division
Newark, NJ 07102

May 26, 1989

Unclassified
SECURITY CLASSIFICATION OF THIS PAGE

REPORT DOCUMENTATION PAGE

Form Approved
OMB No 0704-0188

1a REPORT SECURITY CLASSIFICATION Unclassified	1b RESTRICTIVE MARKINGS
2a SECURITY CLASSIFICATION AUTHORITY	3 DISTRIBUTION/AVAILABILITY OF REPORT
2b DECLASSIFICATION/DOWNGRADING SCHEDULE	
4 PERFORMING ORGANIZATION REPORT NUMBER(S)	5 MONITORING ORGANIZATION REPORT NUMBER(S)
6a NAME OF PERFORMING ORGANIZATION New Jersey Institute of Technology 6b OFFICE SYMBOL (If applicable)	7a NAME OF MONITORING ORGANIZATION
6c ADDRESS (City, State, and ZIP Code) Chemistry Division 323 King Blvd. Newark, NJ 07102	7b ADDRESS (City, State, and ZIP Code)
8a NAME OF FUNDING/SPONSORING ORGANIZATION Office of Naval Research 8b OFFICE SYMBOL (If applicable) ONR	9 PROCUREMENT INSTRUMENT IDENTIFICATION NUMBER
8c ADDRESS (City, State, and ZIP Code) 800 N. Quincy St. Arlington, UA 22217-5000	10 SOURCE OF FUNDING NUMBERS PROGRAM ELEMENT NO / PROJECT NO / TASK NO / WORK UNIT ACCESSION NO

11 TITLE (Include Security Classification)
A Molecular Mechanics Analysis of Molecular Recognition By Cyclodextrin Mimics of Alpha-Chymotrypsin.

12 PERSONAL AUTHOR(S)
C.A. Venanzi, P.M. Canzius, Z. Zhang, J.D. Bunce

13a TYPE OF REPORT	13b TIME COVERED	14 DATE OF REPORT (Year, Month, Day)	15 PAGE COUNT
Manuscript	FROM _____ TO _____	May 26, 1989	44

16 SUPPLEMENTARY NOTATION
Accepted for Publication in Journal of Computational Chemistry

17 COSATI CODES			18 SUBJECT TERMS (Continue on reverse if necessary and identify by block number)
FIELD	GROUP	SUB-GROUP	
07	03		

19 ABSTRACT (Continue on reverse if necessary and identify by block number)

20 DISTRIBUTION/AVAILABILITY OF ABSTRACT ☒ UNCLASSIFIED/UNLIMITED ☐ SAME AS RPT ☐ DTIC USERS	21 ABSTRACT SECURITY CLASSIFICATION Unclassified
22a NAME OF RESPONSIBLE INDIVIDUAL Harold E. Guard	22b TELEPHONE (Include Area Code) (202) 696-4402 22c OFFICE SYMBOL ONR

DD Form 1473, JUN 86 Previous editions are obsolete. SECURITY CLASSIFICATION OF THIS PAGE

J. Comput. Chem., in press

A MOLECULAR MECHANICS ANALYSIS OF MOLECULAR RECOGNITION BY CYCLODEXTRIN MIMICS OF α-CHYMOTRYPSIN

Carol A. Venanzi[1], Preston M. Canzius, Zhifeng Zhang,
and Jeffrey D. Bunce
Department of Chemical Engineering, Chemistry,
and Environmental Sciences
New Jersey Institute of Technology
Newark, NJ 07102

1. Author to whom correspondence should be addressed.

Keywords: Molecular Recognition, Molecular Mechanics, Artificial Enzymes, Enzyme Models, Cyclodextrin, Serine Protease Mimic

ABSTRACT

The method of molecular mechanics is used to investigate the structural and electrostatic features of molecular recognition by β-cyclodextrin and capped β-cyclodextrin models of α-chymotrypsin. Since capped β-cyclodextrin has been shown to be the more effective biomimetic catalyst, these features of molecular recognition can be interpreted in terms of the relationship between molecular structure and catalytic function. Calculations in vacuo show that the addition of an N-methylformamide "cap" substituent to each glucose unit appears to change the relative orientation of some glucose fragments from that found in the X-ray structure of the β-cyclodextrin macrocycle. These results indicate that certain structural components of molecular recognition, such as the orientation of the secondary hydroxyls and the related orientation of the caps, may be implicated in the catalysis.

In addition, the electrostatic component of molecular recognition was investigated by the analysis of molecular electrostatic potential maps calculated in planes parallel to the average plane of the glycosidic oxygen atoms. The results indicate that the addition of the caps to the β-cyclodextrin macrocycle subtly alters the pattern of the maps in each plane. However, the general qualitative features of electrostatic recognition by β-cyclodextrin and capped β-cyclodextrin are similar.

I. INTRODUCTION

Enzymatic catalysis is characterized by substrate specificity and extraordinarily high reaction velocity. In an attempt to elucidate the source of such catalytic efficiency, several laboratories are involved in the design and synthesis of artificial enzymes[1]. These relatively small, non-peptide compounds attempt to reproduce enzymatic reaction rates and substrate specificity by mimicking the molecular recognition features typical of enzyme-substrate interactions. Molecular recognition[2] occurs through the alignment of the complementary shapes as well as the complementary functionalities of the interacting partners: enzyme or enzyme mimic "host" and substrate "guest". At long range, electrostatic interactions influence the selection of the appropriate guest and then orient and direct the guest into the binding site. At short range, complementarity in the molecular shapes of the interacting partners further influences the selection of the guest for the binding site, and leads to favorable van der Waals interactions. In addition, the arrangement of the functional groups of the host must complement the guest in the orientation of charged residues, hydrogen bonding partners, and hydrophobic groups.

For example, functional groups similar to the catalytic residues of enzymes have been added to cyclic urea[3,4], cyclodextrin[5-10], and crown ether[11] macrocyclic templates. In these artificial enzymes, the macrocycles provide the complexation site, while the additional molecular architecture holds the catalytic functional groups in position for optimal interaction with the transition state of the

substrate. In this way, the artificial enzymes provide both shape and functional group complementarity for the substrate.

Recent work in the laboratories of Bender[8,12,13], Breslow[5-7], and Cram[3,4] has focused on the design of compounds that contain functional groups that could mimic the action of the Serine-195, Histidine-57, and Aspartate-102 residues of α-chymotrypsin. Some of these compounds have been shown to approach enzymatic velocities in reactions similar to the acylation and/or deacylation step in the hydrolysis mechanism of chymotrypsin.

For example, the Bender and Breslow groups have independently studied inclusion complexes formed by cyclodextrin hosts and ester guests as models of the enzyme - substrate complex formed during the acyl transfer step initiated by the Ser-195 of chymotrypsin. Bender and coworkers[13] demonstrated that β-cyclodextrin causes a distinct stereoselective acceleration of phenol release from a series of substituted phenyl acetates in alkaline solution. However, the largest rate increase obtained was only 250 times that for nucleophilic attack by a hydroxide ion in the absence of cyclodextrin -- significantly less than enzymatic velocity. However, much improved rates have been demonstrated by the Bender group with an extension of this model to include the imidazole and carboxylate functionalities typical of the catalytic triad of chymotrypsin. This model, β-benzyme, has been shown to catalyze the hydrolysis of esters twice as fast as chymotrypsin[8].

In a different direction, by altering the cyclodextrin binding cavity by "capping" each of the seven glucose units with N-methylformamide and N-ethylformamide substituents, Breslow and coworkers[5]

have improved the rate of acyl transfer by a factor of 10^3. Data from binding and kinetic studies indicates that these "caps" form an intrusive floor which blocks one face of the cyclodextrin cavity from entrance by a substrate and that the floor extends up into the cavity to provide additional binding surfaces for the substrate[5]. This suggests that "capping" makes the cavity shallower, positioning the acyl group of the substrate in a more optimal orientation for interaction with a secondary hydroxyl group on the rim of the cavity. Improved rates of 10^7 compared to unfunctionalized cyclodextrin have also been exhibited by optimization of the substrate geometry to fit the cyclodextrin cavity[5-7]. In these cases, the rate increase was attributed to an improvement in the geometry of the complex to approach that of the transition state.

As part of a concerted program in this laboratory to study enzymatic catalysis at the molecular level by investigating both molecular recognition and the energetics of binding in artificial enzyme systems, we present here our initial studies on molecular recognition by β-cyclodextrin models of chymotrypsin. In this paper, we focus on the relationship between the molecular structure of N-methylformamide "capped" β-cyclodextrin (hepta-N-methylformamide β-cyclodextrin) and its function as a biomimetic catalyst[5]. We use the method of molecular mechanics to investigate the effect of "capping" on the conformation of the β-cyclodextrin macrocycle in order to determine: (1) The molecular structure (shape and extent) of the intrusive floor; (2) The relative flexibility of the glycosidic linkages of the macrocycle; (3) The orientation of the secondary hydroxyl groups around the rim of the macrocycle; and (4) The

electrostatic recognition pattern displayed by the mimic to the approaching substrate. We have used molecular mechanics previously[14-18] to investigate molecular recognition by a series of four cyclic urea compounds designed by Cram and coworkers[3,4] to be "incremental partial mimics" of chymotrypsin. The initial studies described here involve the determination and testing of force field parameters necessary to the description of the β-cyclodextrin and hepta-N-methylformamide β-cyclodextrin models. The calculations are carried out in vacuo. The effect of solvent on molecular conformation and the energetics of substrate binding will be the subject of future publications.

II. METHODS

A. Model Building

β-cyclodextrin (B-CD) and hepta-N-methylformamide β-cyclodextrin (capped B-CD) were analyzed as models of the active site of chymotrypsin. The initial structures of the mimics used as input to the molecular mechanics program AMBER (Assisted Model Building with Energy Refinement)[19] were built using interactive computer graphics and the molecular modeling facility of Chem-X[20]. The modeling was carried out on an Advanced Electronics Design 767 color raster graphics terminal interfaced to a VAX 11/785-750 cluster. The starting structure for the B-CD macrocycle used in the conformational analysis was obtained from the X-ray crystal structure of B-CD complexed with 1,4-diazabicyclo[2.2.2]octane in the presence of 13 water molecules[21] obtained from the Cambridge Crystallographic Database[22].

The first step in the AMBER analysis of B-CD and capped B-CD required the construction of a PREP file containing atomic point charges and "dummy" coordinates for a standard glucose or capped glucose fragment. The coordinates of a glucose fragment (Figure 1) were taken from the X-ray structure of the α- cyclodextrin (A-CD) complex with 1-propanol[23]. Hydrogen atom positions were added using Chem-X. This structure was used as input to the Gaussian80-UCSF[24] program in order to obtain STO-3G united atom "potential-derived"[25] atomic point charges for the glucose fragment.

Since no X-ray nor NMR data were available for the structure of capped B-CD, the geometry of the N-methylformamide substituent was built as follows. The geometry of the N,N-dimethylformamide molecule was built from standard bond angles and bond lengths, and then optimized using the MNDO (Modified Neglect of Diatomic Differential Overlap)[26] method as implemented in the MOPAC program[27]. The capped glucose fragment was constructed by: (1) deleting the C6-O6-H6 fragment from glucose and a hydrogen from a carbon atom of N,N-dimethylformamide; (2) formimg a bond of length 1.497 Å between the C5 of the glucose fragment (described above) and the carbon atom of the formamide fragment (C6 in Figure 2); and (3) setting the C5-C6-N6 bond angle equal to 109.5°, and the C6-N6-C7 and C6-N6-C8 bond angles to 120.0°. This structure was used as input to Gaussian80-UCSF in order to determine STO-3G united atom potential-derived charges for the capped glucose fragment.

The LINK module of AMBER was used to connect the seven fragments into a macrocycle. The EDIT module was used to replace the set of "dummy" B-CD macrocycle coordinates with the coordinates from the

X-ray structure and to add hydrogen atoms at a bond length of 1.0 Å. In the case of capped B-CD, the Cartesian coordinates of the caps were determined by EDIT from the internal coordinates of each cap and its position on a specific glucose fragment of the macrocycle. This resulted in a starting structure for capped B-CD with all the caps placed under the macrocycle (see Figure 3).

The conformational analysis was carried out with version 2.0 of AMBER. A cutoff of 2.0 Å was used for the hydrogen bonding interactions. The 1-4 van der Waals and 1-4 electrostatic scaling parameters and the dielectric constant was set equal to 1.0. The AMBER parameter database was supplemented as described below.

B. Force Field Parameters

The AMBER force field was developed by Kollmann and coworkers to treat proteins and nucleic acids[28], as well as small molecules[29,30]. AMBER approximates the conformational energy of a molecule as the sum of bond stretching, angle bending, torsional, van der Waals, electrostatic and hydrogen bonding interactions. However, angle bending parameters for atom type combinations not provided in the database were needed to describe the cyclodextrin mimics of chymotrypsin. For example, parameters were required for the OS-CH-OS bond angle, where OS is the O4 glycosidic oxygen assigned to one fragment and CH and OS are the C1 carbon and O5 ring oxygen of the neighboring fragment (see Figures 1 and 2). In the AMBER definition of atom types, OS is an ether or ester oxygen and CH is an sp^3 carbon with one "attached" hydrogen in the united atom approximation. Since the AMBER database contained parameters for the central atom, CH, in a similar chemical environment, C2-CH-OS, these parameters (K_θ = 80.0 Kcal/(mol deg)

θ = GREEK SYMBOL THETA

and Θ_{eq} = 109.5°) were used for the OS-CH-OS system. (In the AMBER scheme, C2 is an sp^3 carbon with two "attached" hydrogens in the united atom approximation.)

For capped B-CD, bond angle bending parameters were required for the CH-C2-N and C2-N-C3 angles (C5-C6-N6 and C6-N6-C7 in Figure 2). The atom type N is an sp^2 nitrogen in an amide group and C3 is an sp^3 carbon with three "attached" hydrogens in the united atom approximation. For CH-C2-N the parameters for C2-C2-N (K_Θ = 80.0 Kcal/(mol deg) and Θ_{eq} = 111.2°) from the database were used; for C2-N-C3, the parameters for CH-N-C3 (K_Θ = 50.0 Kcal/(mol deg) and Θ_{eq} = 118.0°) from the database were used.

C. Structural Superposition

In order to test the force field parameters and to investigate the effect of the caps on the conformation of the macrocycle, the minimized structures of B-CD and capped B-CD were separately fit to the coordinates of the macrocycle taken from the X-ray structure of the B-CD complex[21]. Using the RMS fitting facility of AMBER, all 77 atoms (except hydrogens) of B-CD and all 70 atoms (except hydrogens and cap substituents N6, C7, C8, and O8) of capped B-CD were fit to the X-ray structure. Before the structural superposition, the X-ray structure was oriented so that its glycosidic oxygens were in the x-y plane at z = 0 Å.

Since the X-ray structure was used as the starting structure for the energy minimization, there was no ambiguity in the numbering of the glucose fragments: fragment 1 of the X-ray structure corresponded to fragment 1 of the calculated structure, etc. This was not the case for the neutron diffraction structure. In order to be able to make

geometrical comparisons fragment-by-fragment as in the tables in the Results Section, it was necessary to resolve this ambiguity. The fragments of the neutron diffraction structure were arbitrarily numbered from 1 to 7 in consecutive order. Then the two structures were superimposed in seven different ways: (1) fragment 1 (calculated structure) fit to fragment 1 (neutron diffraction structure), fragment 2 to fragment 2, etc.; (2) fragment 1 to fragment 2, fragment 2 to fragment 3, etc.; and so on. From the structural superposition which gave the lowest standard deviation (0.6666) in the root mean square fit, the glucose fragments of the neutron diffraction structure were renumbered to coincide with the numbering scheme of the calculated structure. This numbering scheme is used to present the geometrical information for the neutron diffraction structure in the tables.

D. Molecular Electrostatic Potential

The molecular electrostatic potential was approximated by the Coulombic interaction between a positive point charge and the static charge distribution of the mimic, modeled by the potential-derived atomic point charges positioned at the nuclei. The maps were calculated for the B-CD and capped B-CD macrocycles taken from the structural superposition of Section C. In this orientation, the coordinates of the caps and of the primary hydroxyl groups have positive z values, while the secondary hydroxyls have negative z values. In order to see how the electrostatic recognition pattern of the binding site changed as a substrate approached the secondary hydroxyls from the negative z direction, maps were calculated for a series of x-y planes with negative z values. The Chem-X "Set Dummy" command was used to define the coordinates of a centroid (dummy atom) as the

average x, y, and z positions of the glycosidic oxygens of the mimic. The z-coordinate of the dummy atom was changed from -6.0 Å to 0.0 Å in increments of 2 Å. At each new z-value, the molecular electrostatic potential contour map was calculated by using the "Set Map" facility of Chem-X in which points of equal energy are connected to produce the contours on the map. The contour levels chosen were -50, -30, -10, 0, 10, 30, and 50 Kcal/mol.

III. RESULTS

A. Energy Minimization

The results of the energy minimization of the B-CD and capped B-CD mimics of α-chymotrypsin are presented in Table I. A comparison of the component energies of B-CD (first row) and capped B-CD (second row) indicates that the van der Waals component of the total energy is significantly more negative for capped B-CD than for B-CD. The 1-4 van der Waals term is also larger (more positive) for capped B-CD. The bond stretching, bond angle bending, and hydrogen bonding energies, however, are approximately the same for both mimics. This trend is expected since the addition of the cap substituents provides the potential for additional van der Waals interactions.

The largest difference in energy between the mimics occurs in the electrostatic and 1-4 electrostatic terms which, taken together, account for 147 of the 155 Kcal/mole energy difference. This illustrates the importance of the electrostatic term in determining the conformational energy.

B. Test of Force Field Parameters

In the absence of X-ray and NMR data on the conformation of capped β-cyclodextrin, the chief test of the force field parameters

is the comparison of the calculated B-CD structure to the available structural data on B-CD, much of which has been summarized in a recent review by Saenger[31]. For example, circular dichroism studies[32] have shown that hydrated B-CD, in contrast to A-CD, undergoes very little conformational change upon binding a substrate. This is attributed to the fact that B-CD adopts a "round" structure in solution[33], whereas the A-CD cavity is somewhat "collapsed" due to the rotation inward of one of the glucose units to allow hydrogen bonding between the primary O6 hydroxyl and the included water[34]. The conformational stiffness of the round B-CD is attributed to a network of strong intramolecular hydrogen bonds involving the secondary O2-H and O3-H hydroxyls[33]. A neutron diffraction study of B-CD undecahydrate (B-CD•11H_2O) at 298K[34] has shown that the round structure of the macrocycle is stabilized by a network of "flip-flop" hydrogen bonds between the secondary hydroxyls of consecutive glucose units. The term "flip-flop" hydrogen bond is used to describe a statistical average between the hydrogen bonding arrangements O-H...O and O...H-O, with the oxygen atoms separated by 2.7 - 3.0 Å. At 120K, a neutron diffraction study[36] of B-CD•11H_2O was able to resolve the dynamic "flip-flop" motion into a complex pattern of homodromic (all hydroxyls pointing in the same direction) hydrogen bonds involving the secondary hydroxyls and water molecules both internal and external to the cavity. A pattern of interglucose hydrogen bonds involving the secondary hydroxyls and water was also observed in the X-ray structure of B-CD complexed with 1,4-diazabicyclo[2.2.2]octane[21].

Although the calculations were carried out in the absence of solvent, the demonstrated stiffness of the B-CD macrocycle indicates

that the structure in vacuo should be similar to that of the complexed macrocycle. This is supported by the results of the root mean square fit of the calculated structure to that of the macrocycle taken from the complex with 1,4-diaza[2.2.2]octane[21]. The fit of the 77 (non-hydrogen) atoms of the macrocycle gave a standard deviation of 0.229. The positions of the secondary hydroxyl oxygens are compared to those in the X-ray structure in Table II. The distances in the table are the absolute magnitude of the differences between the atomic positions taken from the superimposed calculated and X-ray structures in the RMS fit. The positions of both the O2 and O3 atoms in each of the seven glucose fragments are very similar to those of the X-ray structure. The largest difference is in fragment 6, with 0.360 Å for the O2 and 0.329 Å for the O3 positions.

The calculated structure of B-CD also shows a network of intramolecular interglucose hydrogen bonds arranged in a homodromic fashion: H2 of fragment 1 is hydrogen bonded to O3 of fragment 2, etc. This is illustrated in Table III. The hydrogen bond lengths range from 1.88 Å to 2.27 Å and agree well with the flip-flop hydrogen bond lengths of 1.89 Å to 2.12 Å from the neutron diffraction study[35] and the hydrogen bond lengths of 1.72 Å to 2.10 Å from the X-ray structure of the B-CD complex[21]. Since discrete solvent molecules were not included in the calculation, more explicit comparison to the neutron diffraction homodromic hydrogen bonding pattern cannot be made, as was possible with a recent molecular dynamics simulation[37,38]. For this reason also, Table VI below does not contain comparisons for torsional angles involving primary or secondary hydroxyl hydrogens.

Selected torsional angles in the calculated structure are compared to those of the neutron diffraction and X-ray structures in Tables IV-VI. Table IV compares the calculated and experimental values for each of the six torsional angles within the glucose ring. The value of the angle is listed for each fragment along with the average value of the angle. The spread of values, defined as the absolute value of the difference between the largest and smallest angles, gives an indication of the variation of the angle over the fragments. The table shows that there is good agreement between the calculated and experimental structures. The average values of the angles C1-O5-C5-C4, C4-C3-C2-C1, C3-C2-C1-O5, and C2-C1-O5-C5 agree to within 1-3^{o} of the average experimental values, while O5-C5-C4-C3 and C5-C4-C3-C2 are within 5 to 7^{o} of the average experimental values. The spread of values for each angle over the fragments is low: ranging from 2.2^{o} for C2-C1-O5-C5 to 5.8^{o} for C5-C4-C3-C2 in the calculated values and up to 9.5^{o} for C1-O5-C5-C4 in the neutron diffraction study. The calculations, therefore, agree with the experimental result[21] that within the β-cyclodextrin macrocycle, the 7 glucose residues are in nearly identical chair conformations.

Table V gives the values of the torsional angle connecting consecutive fragments. Atoms C3, C4, and O4 are on fragment $\underline{i}$, while C1 is on fragment $\underline{i+1}$. The calculated values are generally within range of the experimental values, indicating that the relative orientation of the glucose fragments is similar. The largest difference between the interglucose torsional angles is for the angle connecting fragments 2 and 3. In this case, the values range from 87.1^{o} (X-ray) to 101.9^{o} (calculated) to 130.6^{o} (neutron diffraction) and indicates a

difference in orientation required to bind the substrate, 1,4-diazabicyclo[2.2.2]octane, and included water molecules.

Table VIA reports the torsional angles involving the exocyclic secondary hydroxyl oxygens, O2 and O3. Again, there is good agreement between the calculated and experimental results. This is consistent with the results of Table III since it is the secondary hydroxyl oxygens which are involved in the interglucose hydrogen bonds noted above.

Table VIB reports the torsional angles involving the primary hydroxyl oxygen, O6, for each of the glucose fragments. The difference in the experimental results for fragment 3 (-177.3° in the neutron diffraction study and 58.0° in the X-ray data) is due to a different orientation of the O6-H hydroxyl group in binding a water molecule. In general, the experimental and calculated torsional angles are in good agreement.

These comparisons indicate that the force field used in the calculation can reproduce experimental structural data.

C. Comparison of β-Cyclodextrin and Capped β-Cyclodextrin Structures

The root mean square fit of 70 (non-hydrogen) atoms of the capped B-CD macrocycle to the X-ray structure of B-CD gave a standard deviation of 0.815. This is larger than the value for the calculated B-CD/X-ray fit described in Section B and indicates that, in the absence of solvent, the addition of caps changes the orientation of the glucose units of the β-cyclodextrin macrocycle from that in the X-ray structure. This can be seen in more detail from the analysis of the orientation of the secondary hydroxyl oxygens, the hydrogen

bonding pattern, and the torsional angles of capped β-cyclodextrin in Tables II-VI.

Table II gives the difference in the positions of the secondary hydroxyl oxygens of capped B-CD compared to those in the X-ray structure. In general, these differences are significantly larger than the values for B-CD shown in the second and third columns of the table. The largest position differences are for fragments 1 (1.431 Å and 1.514 Å compared to 0.205 Å and 0.160 Å), 4 (2.327 Å and 2.239 Å compared to 0.195 Å and 0.056 Å), and 6 (1.109 Å and 0.771 Å compared to 0.360 Å and 0.329 Å). This seems to indicate that the addition of the caps to the glucose fragments of the macrocycle causes a significant change in the orientation of the secondary hydroxyl oxygens of fragments 1, 4, and 6. This can be seen in more detail in Figure 4. Figure 4A displays the calculated structure of B-CD in the orientation obtained after fitting to the X-ray structure. Figure 4B shows the structure of capped B-CD obtained from a similar fit to the X-ray structure. Both figures give the fragment number in parentheses. From a comparison of Figures 4A and 4B, it can be seen that in fragments 1 and 4 the caps move out (away from under the macrocycle) causing the secondary hydroxyls to move in toward the center of the cavity. In fragment 6, the secondary hydroxyls move out, while the caps move in, forming a floor to the cavity. Figures 4A and 4B show that the glucose units of fragments 2, 3, 5, and 7 appear to be in the same orientation. This agrees with the data in Table II which shows that the smallest differences in the O2 and O3 positions occur for these fragments.

Table III gives the distances between atom H2 of fragment i+1 and atom O3 of fragment i in capped B-CD. The homodromic hydrogen bonding network is very similar to that of B-CD, except for the larger values of 2.38 Å and 3.31 Å involving fragment 6. Figure 4 has already illustrated how fragment 6 is twisted so that its secondary hydroxyls move out, away from under the macrocycle relative to B-CD. This, then, is the cause of the disruption of the hydrogen bonding network. In fact, fragment 6 is twisted to such a degree that its H2 atom is almost as close to the glycosidic O4 of fragment 5 (2.46 Å) as it is to the O3 atom of fragment 5 (2.38 Å).

The twisting of fragment 6, as well as fragments 1 and 4, noted in Figure 4 is substantiated by the interglucose torsion angle data in Table V. The largest differences in the capped B-CD torsion angles compared to B-CD are for angles involving fragments 1, 4, and 6. For example, the 7-1 torsional angle is 86.3° in capped B-CD, but 114.6° in B-CD. The 3-4 angle is 83.3° in capped B-CD, but 128.8° in B-CD. And the 5-6 torsional angle is 154.7° in capped B-CD, but 137.6° in B-CD.

However, Table IV shows that the cap substituents have a small effect on the internal glucose torsional angles. The average values reported for capped B-CD are very close to those calculated for B-CD for each angle. However, the spread of values for each angle is larger in capped B-CD, reaching 16.8 and 15.5 for O5-C5-C4-C3 and C5-C4-C3-C2, respectively.

Table VI presents the effect of the caps on the exocyclic primary and secondary hydroxyl oxygen positions. Table VIA shows that there is little change in the exocyclic torsion angles involving the

secondary hydroxyl oxygens compared to B-CD. However, Table VIB shows generally large changes in the angle C4-C5-C6-N6, involving the nitrogen of the cap, compared to angle C4-C5-C6-O6 in B-CD. This agrees with the general reorientation of the caps shown in Figure 4.

D. Molecular Recognition by Electrostatic Complementarity

The general electrostatic recognition pattern of the cyclodextrins was investigated by analysis of two-dimensional molecular electrostatic potential contour maps. The atomic point charges used in the calculation are given in Table VII. Comparison of the charges in columns 2 and 3 show that the charges of the glucose atoms (C1 through O4) are very similar for both the glucose and capped glucose fragments. The atoms close to the point of attachment of the cap (O5, C5, C6, C4) show the largest difference in charge (0.04 - 0.05) between the glucose and capped glucose fragments.

The molecular electrostatic potential contour map for B-CD in the x-y plane at z = 0 Å is presented in Figure 5. The potential map of the macrocyclic cavity appears to be very positive and symmetrical with contours of 30 and 50 Kcal/mol within the perimeter of the cavity and 0 and 10 Kcal/mol in the external region. The map shows only one small contour of -10 Kcal/mol in the lower left-hand corner of the figure. At z = - 2.0 Å (not shown), a plane which is near the secondary hydroxyls on the rim of the cavity, the features of the map are essentially the same as at z = 0 Å. However, from the region external to the perimeter of the cavity, several contours at -10, -30, and -50 Kcal/mole appear. At z = -4 Å (not shown), the map contours are generally positive and symmetric, the chief feature being a contour of 10 Kcal/mol which follows the shape of the cavity. A few small

contours of -10 Kcal/mol and one contour of -30 Kcal/mol appear in the region external to the perimeter of the cavity. At -6.0 Å (not shown), the map shows only a single contour level of 0 Kcal/mol.

The maps show that a substrate approaching from the negative z direction would be presented with a generally positive and symmetric electrostatic potential pattern by the B-CD macrocycle. The maps show that the strength of the interaction would increase as the substrate approached the cavity. The "bull's eye" nature of the pattern would assist in directing a substrate approaching from an arbitrary direction into the binding cavity. The maps give a qualitative indication of the complementary electrostatic potential pattern that must be presented to the cyclodextrin mimic by a suitable substrate.

The molecular electrostatic potential contour map for capped B-CD at z = 0 Å is presented in Figure 6. Within the perimeter of the cavity, the features of the capped B-CD map are very similar to those of the B-CD map at z = 0 Å. The chief features are contours of 30 and 50 Kcal/mol, which give a positive and symmetric pattern to the map. The map differs in the regions where fragments where fragments 1, 4, and 6 are twisted from their orientation in B-CD. In these areas, negative contours of -10, -30, and -50 Kcal/mol appear due to the proximity of the atoms of the secondary hydroxyls of fragments 1, 4, and 6 to the plane in which the map is calculated.

At z = - 2.0 Å (not shown), the map is very similar to that of B-CD at z = - 2.0 Å, showing contours of 30 and 50 Kcal/mol within the perimeter of the cavity. Contours of -10 and -30 Kcal/mol appear in the areas around fragments 2, 3, 5, and 7. This is due to the fact that the hydroxyl groups of these fragments are near the plane in

which the map was calculated. The regions around fragments 1, 4, and 6 appear more positive in the capped B-CD map than in the B-CD map because the hydroxyls of the fragments are further from the plane containing the map.

At z = -4.0 Å (not shown), the map of capped B-CD is similar to B-CD within the perimeter of the cavity, with contours of 10 and 30 Kcal/mol presenting a positive recognition pattern. The area external to the perimeter of the cavity also presents a positive and symmetric pattern, distinguished by contours at 0 and 10 Kcal/mol. This differs from the B-CD map at -4.0 Å which had several contours of -10 and -30 Kcal/mol in the region external to the cavity.

At z = -6.0 Å, the map is similar to that of B-CD in that it is symmetrical. The capped B-CD map is more positive, however, with a large contour of 10 Kcal/mol outlining the perimeter of the cavity.

In general, the chief features of the B-CD and capped B-CD molecular electrostatic potential maps are very similar. The maps are characterized by a positive and symmetric pattern within the cavity which is distinguishable at all the distances studied, as well as negative contours in the planes containing the secondary hydroxyl groups. This suggests that, although the caps alter the conformational properties of the B-CD macrocycle, they do not significantly alter the long - range electrostatic potential pattern presented to the substrate.

IV. DISCUSSION

An important test of any force field is its ability to reproduce experimental data. In the calculated structure of B-CD, the homodromic hydrogen bond pattern (Table III) between the secondary

hydroxyls of adjacent glucose units reproduced the general features of the hydrogen bonding pattern observed in the X-ray and neutron diffraction data. However, since water molecules were not included in the calculation, the results cannot show the detailed hydrogen bonding network involving hydroxyl hydrogens and solvent displayed in the neutron diffraction data[36] and molecular dynamics simulations[37,38].

The force field was also able to reproduce the general features of the orientation of the secondary hydroxyl oxygens of B-CD (Table II), as well as the internal glucose (Table IV) and exocyclic torsional angles involving the primary and secondary hydroxyl oxygens (Table VI). In particular, the calculated interglucose torsional angles (Table V) were close to the experimental values. This supports the choice of the OS-CH-OS bond angle bending parameters used to supplement the AMBER force field.

The large rate acceleration of capped B-CD compared to B-CD in acyl transfer reactions has been attributed[5] to the formation of an intrusive floor by the caps. This floor, by making the cyclodextrin cavity shallower, may allow the substrate to bind in an orientation similar to that of the transition state of the complex. The present work has begun to explore the molecular orientation of the floor formed by the caps. From a starting structure in which all the caps were placed under the macrocycle, the caps of fragments 1 and 4 moved out, twisting the glucose fragments and turning the corresponding secondary hydroxyls in toward the center of the cavity. Conversely, the secondary hydroxyls of fragment 6 moved out, while the cap moved in, covering part of the cavity. This may indicate that there is too much steric hindrance for all the caps to be under the macrocycle

simultaneously. In order to determine whether these effects are an artifact of the choice of starting structure for the minimization procedure, distance geometry[39] is being used to generate new starting structures for additional molecular mechanics analysis. Similarly, the effect of solvent on the orientation of the "caps" is being explored through molecular dynamics simulation.

The present results show that the reorientation of the caps affects the position of the secondary hydroxyls such that some of them point in towards the center of the cavity. This suggests the possibility that the observed rate enhancement may be due to a combination of factors: the partial floor forces the substrate up towards the rim, while at the same time, a hydroxyl group is moved in towards the substrate, facilitating an arrangement close to the geometry of the transition state of the complex. Additional molecular mechanics studies of the mimic - substrate complex are being carried out in this laboratory to explore this hypothesis.

Recently, in separate molecular mechanics studies using the MacroModel[40] program with the MM2 force field option supplemented with parameters for ferrocene substrates, the Menger[41] and Breslow[42] groups concluded that the very high rate acceleration exhibited by the p–nitrophenyl ester of ferrocenylacrilic acid, compared to other substrates, was not due to differences in initial binding geometries. Rather, distortion in the ester linkage of the cyclodextrin "acyl–enzyme" model was seen to destabilize the product and lower the acceleration for leaving groups poorer than p–nitrophenyl. Work is in progress to examine these effects for substrate binding to capped cyclodextrin.

In summary, the results presented here suggest that certain structural features of molecular recognition may be altered by the addition of cap substituents to the B-CD macrocycle. Comparison of the B-CD and capped B-CD structures calculated in vacuo shows differences in the orientation of the secondary hydroxyls due to twisting of some of the glucose fragments to avoid unfavorable steric interactions. These structural components of molecular recognition may be implicated in the catalysis since the secondary hydroxyl oxygen mimics the Ser-195 of chymotrypsin in initiating the acyl transfer event through nucleophilic attack on the substrate. This will be further explored through studies on the effect of solvent and included substrate on the conformation of the B-CD macrocycle.

In contrast, comparison of the molecular electrostatic potential patterns of B-CD and capped B-CD showed that the qualitative features of electrostatic recognition are similar in both macrocycles. The addition of the cap substituents caused only subtle alteration of the molecular electrostatic recognition pattern.

ACKNOWLEDGEMENTS

This work has been supported by grants to C.A.V. from the National Science Foundation (CPE-8404363), the Donors of the Petroleum Research Fund of the American Chemical Society, the New Jersey Commission on Science and Technology, the Office of Naval Research, and the Hoffmann LaRoche, Ciba-Geigy, and Schering-Plough Corporations. C.A.V. acknowledges a generous grant of computer time from New Jersey Institute of Technology.

REFERENCES

1. See, for example: (a) H. Dugas and C. Penny, Bioorganic Chemistry: A Chemical Approach to Enzyme Action, Springer-Verlag: New York, 1981, Chapter 5; (b) Biomimetic Chemistry, Advances in Chemistry 191, D. Dolphin, C. McKenna, Y. Murakami, and I. Tabushi, Eds.; American Chemical Society, Washington, D. C. 1980; (c) Design and Synthesis of Organic Molecules Based on Molecular Recognition, G. van Binst, Ed., Springer-Verlag, Berlin, 1986; (d) The Bioorganic Chemistry of Enzymatic Catalysis, M. L. Bender, R. J. Bergeron, and M. Komiyama, Eds., John Wiley and Sons, New York, 1984.
2. J. Rebek, Jr., in: Molecular Structure and Energetics, **10**, J. F. Liebman and A. Greenberg, Eds., VCH, New York, p. 219-250.
3. D. J. Cram and H. E. Katz, J. Am. Chem. Soc., **105**, 135 (1983).
4. D. J. Cram, P. Y.-S. Lam, and S. P. Ho, J. Am. Chem. Soc., **108**, 839 (1986).
5. R. Breslow, M. F. Czarniecki, J. Emert, and H. Hamaguchi, J. Am. Chem. Soc., **102**, 762 (1980).
6. G. L. Trainor and R. Breslow, J. Am. Chem. Soc., **103**, 158 (1981).
7. R. Breslow, G. Trainor, and A. Ueno, J. Am. Chem. Soc., **105**, 2739 (1983).
8. V. T. D'Souza, K. Hanabusa, T. O'Leary, R. C. Gadwood, and M. L. Bender, Biochem. Biophys. Res. Commun., **129**, 727 (1985).
9. (a) R. Breslow, A. W. Czarnick, M. Lauer, R. Leppkes, J. Winkler, and S. Zimmerman, J. Am. Chem. Soc., **108**, 1969 (1986); (b) W. Weiner, J. Winkler, S. C. Zimmerman, and R. Breslow, J. Am. Chem. Soc., **107**, 4093 (1985); (c) For a review, see: R. Breslow, in:

Inclusion Compounds, 3, J. L. Atwood, J. E. D. Davies, and D. D. MacNicol, Eds., Academic Press, New York, 1984, Chapter 14.

10. I. Tabushi, Y. Kuroda, and I. Mochizuki, J. Am. Chem. Soc., 102, 1152 (1980).
11. J. P. Behr, J. M. Lehn, D. Moras, and J. C. Thierry, J. Am. Chem. Soc., 103, 701 (1981).
12. I. M. Mallick, V. T. D'Souza, M. Yamaguchi, J. Lee, P. Chalabi, R. C. Gadwood, and M. L. Bender, J. Am. Chem. Soc., 106, 7252 (1984).
13. (a) R. L. van Etten, G. A. Clowes, J. F. Sebastian, and M. L. Bender, J. Am. Chem. Soc., 89, 3242 (1967); (b) ibid., 3253 (1967).
14. C. A. Venanzi and J. D. Bunce, Int. J. Quantum Chem., QBS12, 69 (1986).
15. C. A. Venanzi and J. D. Bunce, Ann. N. Y. Acad. Sci., 471, 318 (1986).
16. C. A. Venanzi and J. D. Bunce, Enzyme, 36, 79 (1986).
17. C. A. Venanzi, in: Molecular Structure and Energetics, 10, J. F. Liebman and A. Greenberg, Eds., VCH, New York 1989 , p. 251-279.
18. C. A. Venanzi and K. Namboodiri, Anal. Chim. Acta, 210, 151 (1988).
19. P. K. Weiner and P. A. Kollman, J. Comput. Chem., 2, 287 (1981).
20. Chem-X, developed and distributed by Chemical Design, Ltd., Oxford, England.
21. K. Harata, Bull. Chem. Soc. Jpn., 55, 2315 (1982).
22. F. H. Allen, O. Kennard, and R. Taylor, Acc. Chem. Res., 16, 146 (1983).
23. W. Saenger, R. K. McMullen, J. Fayos, D. Mootz, Acta Cryst. B30,

2019 (1974).

24. U. C. Singh and P. Kollman, QCPE Bull., 2, 17 (1982).
25. U. C. Singh and P. Kollman, J. Comput. Chem., 5, 129 (1984).
26. M. S. Dewar and W. Thiel, J. Am. Chem. Soc., 99, 4899 (1977).
27. J. J. P. Stewart, QCPE Bull., 3, 43 (1983).
28. S. J. Weiner, P. A. Kollman, D. A. Case, U. C. Singh, G. Alagona, S. Profeta, Jr., and P. Weiner, J. Am. Chem. Soc., 106, 765 (1984).
29. G. Wipff, P. Weiner, and P. Kollman, J. Am. Chem. Soc., 104, 3249 (1982).
30. P. A. Kollman, G. Wipff, and U. C. Singh, J. Am. Chem. Soc., 107, 2212 (1985).
31. W. Saenger, in: Inclusion Compounds, 2, J. L. Atwood, J. E. D. Davies, D. D. MacNicol, Eds., Academic Press, New York, 1984, Chapter 8.
32. D. A. Rees, J. Chem. Soc. B, 877 (1970).
33. K. Lindner and W. Saenger, Carbohydr. Res., 107, 7 (1982).
34. B. Klar, B. Hingerty, and W. Saenger, Acta Crystallogr., B36, 1154 (1980).
35. C. Betzel, W. Saenger, B. E. Hingerty, and G. M. Brown, J. Am. Chem. Soc., 106, 7545 (1984).
36. V. Zabel, W. Saenger, and S. A. Mason, J. Am. Chem. Soc., 108, 3664 (1986).
37. J. Koehler, W. Saenger, and W. F. van Gunsteren, Eur. Biophys. J., 15, 211 (1987).
38. J. E. H. Koehler, W. Saenger, and W. F. van Gunsteren, Eur. Biophysics J., 16, 153 (1988).
39. G. M. Crippen, J. Comput. Phys., 24, 96 (1977).

40. W. Clark Still, Columbia University.

41. F.M. Menger and M.J. Sherrod, J. Am. Chem. Soc., **110**, 8606 (1988).

42. H.-J. Thiem, M. Brandl, and R. Breslow, J. Am. Chem. Soc., **110**, 8612 (1988).

Legend to Figures

Figure 1. Atom labelling scheme for glucose fragment; united atom approximation. Atoms C1, C2, C3, C4, and C5 are AMBER atom type CH; O2, O3, and O6 are type OH; H2, H3, and H6 are type HO; O4 and O5 are OS; and C6 is type C2.

Figure 2. Atom labelling scheme for "capped" glucose fragment; united atom approximation. Atom types are the same as in Fig.1 with the addition of N6 (type N), C7 (type C3), C8 (type C), and O8 (type O).

Figure 3. Starting structure for minimization of the "capped" β-cyclodextrin macrocycle.

Figure 4A. Structure of β-cyclodextrin after minimization and superposition onto X-ray structure. Secondary hydroxyl oxygens are labelled. Fragment number is given in parentheses.

Figure 4B. Structure of "capped" β-cyclodextrin after minimization and superposition onto X-ray structure. Secondary hydroxyl oxygens are labelled. Fragment number is given in parentheses.

Figure 5. Molecular electrostatic potential of β-cyclodextrin in the x-y plane at z = 0 Å. The structure of the macrocycle

is superimposed on the map.

Figure 6. Molecular electrostatic potential of "capped" β-cyclodextrin in the x-y plane at z = 0 Å. The structure of the macrocycle is superimposed on the map.

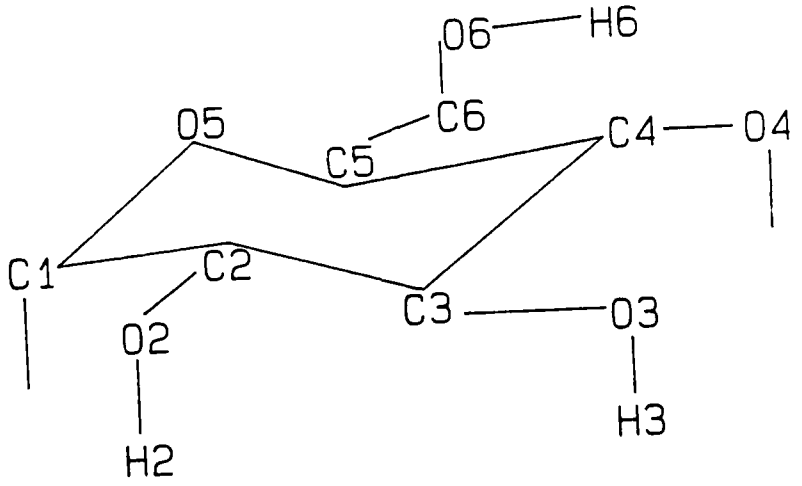

Fig. 1

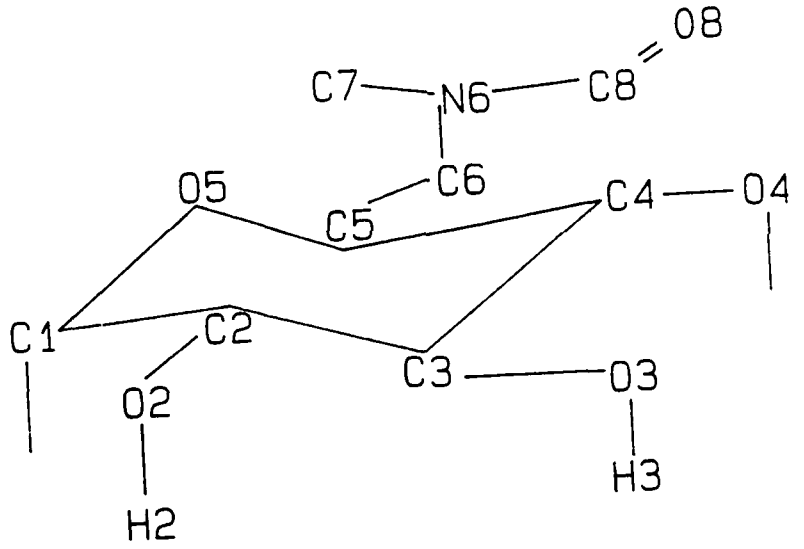

Fig. 2

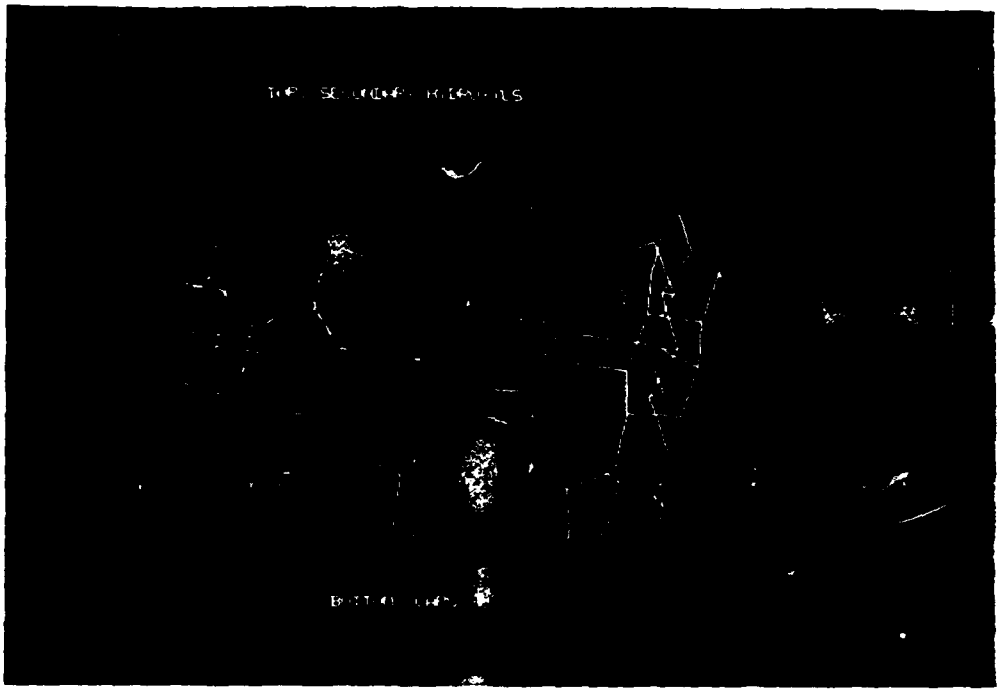

FIG. 3

FIG. 4A

FIG. 4B

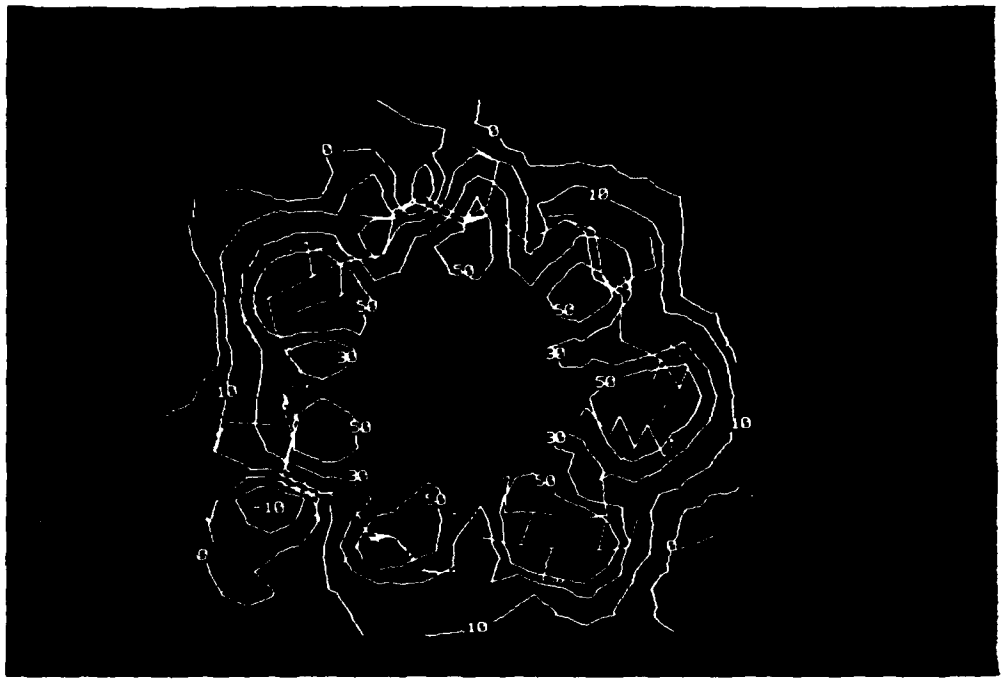

FIG. 5

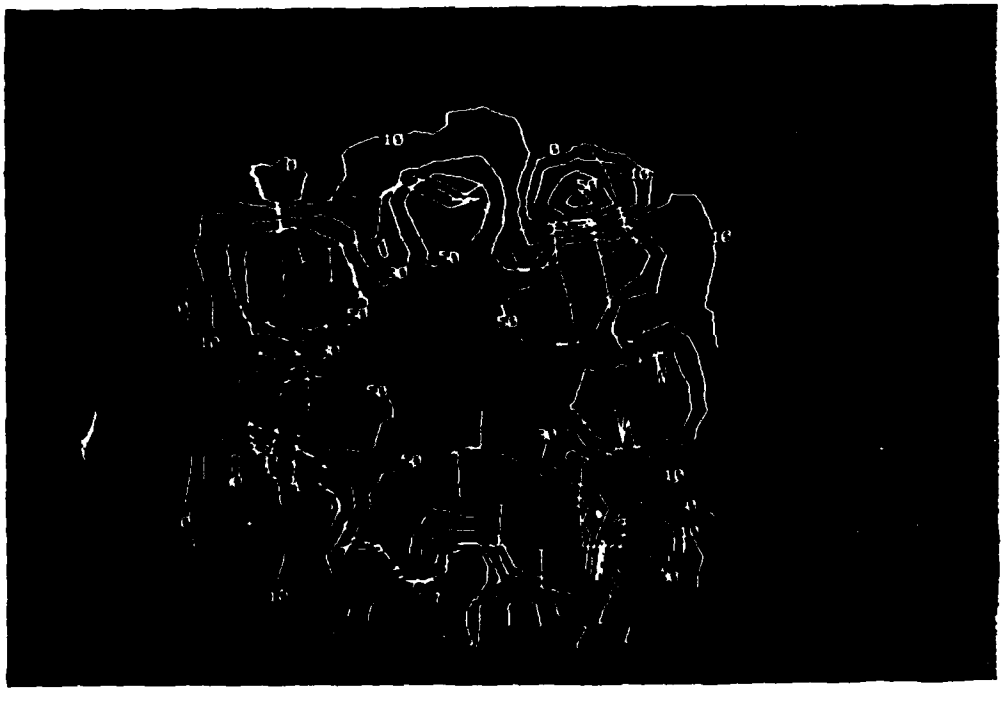

FIG. 6

Table I. Conformational Energy of Cyclodextrins

	Total[a]	Bond	Angle	Dih.	Van der Waals	Elec.	HB	1-4 VDW	1-4 Elec.
B-CD	461.5	4.3	9.2	69.1	-24.5	-477.4	-5.4	17.9	868.3
Capped B-CD	306.5	4.6	12.8	60.1	-39.3	-530.3	-4.0	28.4	774.2

a. Total energy (in units of Kcal/mol) is broken down into bond stretching, angle bending, dihedral angle, van der Waals, electrostatic, hydrogen bond, 1-4 van der Waals, and 1-4 electrostatic contributions.

Table II. Comparison of Calculated and X-ray[a] Secondary Hydroxyl Oxygen Positions[b]

Fragment Number	B-CD		Capped B-CD	
	O2	O3	O2	O3
1	0.205	0.160	1.431	1.514
2	0.127	0.235	0.496	0.627
3	0.170	0.248	0.251	0.197
4	0.195	0.056	2.327	2.239
5	0.166	0.154	0.412	0.515
6	0.360	0.329	1.109	0.771
7	0.189	0.224	0.608	0.631

a. The X-ray coordinates are taken from references 21 and 22.
b. Distances (in Angstroms) are calculated as the absolute value of the difference between the calculated and X-ray positions after structural superposition (see text).

Table III. Interglucose Hydrogen Bonds

Fragments[a]	Hydrogen Bond Distance[b]	
	B-CD	Capped B-CD
1 - 2	1.89	1.92
2 - 3	1.94	1.95
3 - 4	1.88	1.86
4 - 5	2.00	1.89
5 - 6	2.27	2.38
6 - 7	1.92	3.31
7 - 1	1.90	1.93

a. Hydrogen bonds are formed between atom H2 of fragment i+1 and atom O3 of fragment i.
b. Distance given in Angstroms.

Table IV. Comparison of Glucose Internal Torsional Angles

		β-Cyclodextrin			Capped B-CD
Angle[a]	Fragment	Neutron[b]	X-ray[c]	Calculated	Calculated
C1-O5-C5-C4	1	60.9	61.3	58.0	63.0
	2	61.4	57.5	59.1	62.3
	3	56.4	64.3	60.3	59.8
	4	58.0	60.4	56.2	61.9
	5	64.6	60.7	61.1	62.3
	6	61.8	61.2	60.7	64.7
	7	55.1	58.6	58.9	56.3
Average		59.3	60.6	59.2	61.5
Spread[d]		9.5	6.9	4.9	8.3
O5-C5-C4-C3	1	-57.2	-55.3	-47.7	-54.6
	2	-58.1	-52.5	-47.2	-46.1
	3	-50.2	-61.7	-51.3	-46.1
	4	-53.1	-56.8	-47.9	-55.4
	5	-59.4	-55.9	-52.6	-47.6
	6	-55.6	-56.2	-51.9	-56.8
	7	-49.7	-56.3	-48.3	-39.9
Average		-54.7	-56.4	-49.6	-49.5
Spread		8.4	9.2	5.4	16.9

Table IV. (continued)

C5-C4-C3-C2	1	54.6	53.0	47.5	50.8
	2	56.3	53.5	45.1	39.9
	3	51.1	57.8	49.6	43.2
	4	54.2	56.3	49.6	54.6
	5	54.2	55.4	50.9	44.1
	6	53.5	54.0	49.6	50.9
	7	51.2	57.5	46.2	39.1
Average		53.6	55.4	48.3	46.1
Spread		5.1	4.8	5.8	15.5
C4-C3-C2-C1	1	-53.6	-53.6	-52.5	-50.9
	2	-54.7	-54.7	-50.4	-44.6
	3	-54.7	-52.6	-51.6	-48.9
	4	-56.3	-55.7	-54.8	-51.0
	5	-50.1	-55.2	-52.0	-50.0
	6	-53.6	-54.1	-51.0	-48.7
	7	-53.6	-57.7	-49.7	-49.6
Average		-53.8	-54.8	-51.7	-49.1
Spread		6.2	5.2	5.1	6.3

Table IV. (continued)

C3-C2-C1-O5	1	55.1	56.6	58.0	54.3
	2	55.4	58.9	58.1	55.9
	3	58.6	53.0	55.8	57.7
	4	58.7	57.0	59.3	55.3
	5	51.7	57.8	56.0	59.1
	6	56.6	56.2	56.2	51.8
	7	58.0	57.7	56.3	61.0
Average		56.3	56.7	57.1	56.4
Spread		7.0	5.9	3.4	9.2
C2-C1-O5-C5	1	-60.3	-61.6	-63.4	-62.5
	2	-59.5	-61.5	-64.7	-67.4
	3	-60.8	-60.7	-62.8	-65.5
	4	-60.8	-61.0	-62.5	-61.3
	5	-60.0	-61.8	-63.6	-67.9
	6	-62.9	-60.5	-63.6	-61.7
	7	-59.7	-59.2	-63.5	-67.2
Average		-60.6	-60.9	-63.5	-64.8
Spread		3.5	2.6	2.2	6.6

a. In degrees. See Figures 1 and 2 for atom labelling scheme.
b. From references 22 and 35.
c. From references 22 and 21.
d. Spread is defined as the absolute value of the difference between the largest and smallest angles.

Table V. Interglucose Torsional Angles

		β-Cyclodextrin			Capped B-CD
Angle[a]	Fragment	Neutron[b]	X-ray[c]	Calculated	Calculated
C3-C4-O4-C1	1 - 2	125.4	137.3	134.7	137.3
	2 - 3	130.6	87.1	101.9	98.6
	3 - 4	114.2	128.8	128.8	83.3
	4 - 5	140.3	133.4	134.4	125.3
	5 - 6	134.3	132.1	137.6	154.7
	6 - 7	119.0	113.4	100.2	106.4
	7 - 1	129.8	123.2	114.6	86.3

a. In degrees. See Figures 1 and 2 for atom labelling scheme. Torsional angle involving atoms C3, C4, and O4 of fragment i and atom C1 of fragment $i+1$.
b. From references 22 and 35.
c. From references 22 and 21.

Table VI. Exocyclic Torsional Angles

A. Involving Secondary Hydroxyl Oxygens

		β-Cyclodextrin			Capped B-CD
Angle[a]	Fragment	Neutron[b]	X-ray[c]	Calculated	Calculated
O5-C1-C2-O2	1	-179.9	-183.1	-179.6	-182.1
	2	-179.7	-177.7	-176.1	-178.3
	3	180.0	174.0	178.2	180.5
	4	-178.6	-182.7	-176.5	-182.7
	5	175.0	180.7	179.2	186.3
	6	177.6	178.8	179.7	176.6
	7	-179.4	-179.1	-181.6	-176.0
C1-C2-C3-O3	1	-174.9	-173.5	-176.0	-173.3
	2	-176.6	-175.0	-174.0	-167.8
	3	-176.1	-173.2	-175.7	-173.6
	4	-175.7	-173.8	-177.4	-179.0
	5	-174.9	-174.3	-175.7	-172.5
	6	-171.9	-172.8	-174.7	-172.6
	7	-175.0	-178.4	-173.7	-173.9

a. In degrees. See Figures 1 and 2 for atom labelling scheme.
b. From references 22 and 35.
c. From references 22 and 21.

Table VI. (continued)

B. Involving Primary Hydroxyl Oxygens

		β-Cyclodextrin			Capped B-CD
Angle[a]	Fragment	Neutron[b]	X-ray[c]	Calculated	Calculated
C4-C5-C6-O6	1	58.3	54.4	61.6	-164.3
(B-CD)	2	50.3	59.6	63.2	-171.0
	3	-177.3	58.0	64.6	-164.8
or	4	57.1	58.4	64.4	-159.7
	5	-168.8	-172.4	-165.7	-170.4
C4-C5-C6-N6	6	-174.4	-175.5	-162.7	-169.3
(capped B-CD)	7	60.6	54.4	62.6	-168.1

a. In degrees. See Figures 1 and 2 for atom labelling scheme.
b. From references 22 and 35.
c. From references 22 and 21.

Table VII. Atomic Point Charges[a]

Atom	Charge	
	Glucose	Capped Glucose
C1	0.1779	0.1481
C2	0.2687	0.2375
O2	-0.5452	-0.5316
H2	0.2670	0.2706
C3	0.4826	0.5029
O3	-0.5852	-0.5605
H3	0.2970	0.2830
O5	-0.5027	-0.4474
C5	0.3887	0.4459
C6	0.1661	0.1226
C4	-0.0696	-0.1140
O4	-0.1664	-0.1863
O6	-0.4991	------
H6	0.3200	------
N6	------	-0.4490
C7	------	0.2037
C8	------	0.4728
O8	------	-0.3983

a. Potential derived charges, STO-3G basis set, united atom approximation.
b. See Figures 1 and 2 for atom labelling scheme.

DL/1113/89/1

TECHNICAL REPORT DISTRIBUTION LIST, GENERAL

	No. Copies
Office of Naval Research Chemistry Division, Code 1113 800 North Quincy Street Arlington, VA 22217-5000	3
Commanding Officer Naval Weapons Support Center Attn: Dr. Bernard E. Douda Crane, IN 47522-5050	1
Dr. Richard W. Drisko Naval Civil Engineering Laboratory Code L52 Port Hueneme, California 93043	1
Defense Technical Information Center Building 5, Cameron Station Alexandria, Virginia 22314	2 high quality
David Taylor Research Center Dr. Eugene C. Fischer Annapolis, MD 21402-5067	1
Dr. James S. Murday Chemistry Division, Code 6100 Naval Research Laboratory Washington, D.C. 20375-5000	1
Dr. Ronald L. Atkins Chemistry Division (Code 385) Naval Weapons Center China Lake, CA 93555-6001	1
Chief of Naval Research Special Assistant for Marine Corps Matters Code 00MC 800 North Quincy Street Arlington, VA 22217-5000	1
Dr. Bernadette Eichinger Naval Ship Systems Engineering Station Code 053 Philadelphia Naval Base Philadelphia, PA 19112	1
Dr. Sachio Yamamoto Naval Ocean Systems Center Code 52 San Diego, CA 92152-5000	1
David Taylor Research Center Dr. Harold H. Singerman Annapolis, MD 21402-5067 ATTN: Code 283	1